SUPPORTING INFORMATION

Conjugated microporous polymers bearing phosphonate ligands as an efficient sorbent for potential uranium extraction from high-level liquid wastes

Meiyun Xu [a], Xiaoli Han [a], Tao Wang [a], Shenhua Li [a], Daoben Hua [a,b*]

[a] State Key Laboratory of Radiation Medicine and Protection, School of Radiological and Interdisciplinary Sciences (RAD-X), Soochow University, Suzhou 215123, China; correspondence to: dbhua_lab@suda.edu.cn;

[b] Collaborative Innovation Center of Radiological Medicine of Jiangsu Higher Education Institutions, Suzhou 215123, China.

Table of contents

Methods. Transmission electron microscopy (TEM) was performed on a Tecnai G2 spirit BioTwin field emission scanning electron microscope. X-ray photoelectron spectroscopy (XPS) was carried out by an ESCALAB 250Xi spectrometer. Fourier transform infrared (FTIR) spectra were recorded on a Varian-1000 spectrometer. Solid-state ^{13}C CP/MAS NMR measurements were carried out on a Bruker Avance III model 400 MHz NMR spectrometer at a MAS rate of 5 kHz. Surface areas and pore size distributions were measured by N_2 sorption and desorption at 77.3 K using the ASAP 2020 volumetric sorption analyzer. BET surface areas were calculated over the relative pressure range 0.05-0.15 P/P_0. Samples were degassed at 100 °C for 10 h under high vacuum before analysis. Atomic force microscope (AFM) were obtained with a Bruker Multimode 8 scanning probe microscope, operating in tapping mode with phosphorus-doped Si tips (RTESPW, Bruker). CMP-EP was dispersed in ethanol *via* sonication for 1 hour prior to AFM measurement. The concentration of uranium (VI) was determined by thermo high-resolution inductively coupled plasma mass spectrometry (ICP-MS, Element II). ^{60}Co gamma-ray irradiation was carried out at ^{60}Co radiation laboratory of Soochow University and institute of radiation technology of Soochow University.

Synthesis of monomer F-2. 2, 7-dibromo-9, 9'-bis(3-bromopropyl)-fluorene (F-1) were prepared according to reported literatures.[1, 2] F-1 (808.4 mg, 1.43 mmol) was refluxed in triethyl phosphite (10 mL) for 5 hours. After cooling down to room temperature, triethyl phosphite was removed through vacuum distillation. The residual was purified by flash column chromatography (4% ethanol in CH_2Cl_2) to give F-2 (933.2 mg) in 96% yield. 1H NMR ($CDCl_3$, 400 MHz), δ 7.47 (6H, m), 3.92 (8H, m), 1.47 (4H, m), 1.17 (12H, t, J = 7.0 Hz), 0.85 (4H, m).[3]

Synthesis of CMP-H. Nitrogen was bubbled to the DMF solution (50mL) of TBB (187.6 mg, 0.41 mmol) and 2, 7-dibromo-9H-fluorene (200 mg, 0.62 mmol) for 30 min. $Pd(PPh_3)_4$ (31 mg, 0.03 mmol) was added into the solution followed by injection of 1 M Na_2CO_3. The reaction mixture was stirred at a predetermined temperature under N_2. After cooling down, the mixture was centrifugated (4000 rpm, 30 min), and then washed with DMF for 5 times and CH_2Cl_2 for 4 times to remove unreacted monomers and impurities. The residual was dialyzed (MWCO: 8000~14000), and then freeze dried to give CMP-H (115 mg) in 87.7% yield as a white powder.

Sorption kinetics. Pseudo-first-order equation is described as following Equation (1):

$$\log(q_e - q_t) = \log q_e - (\frac{k_1}{2.303}) \times t \qquad (1)$$

where q_e and q_t (mg g^{-1}) are the sorption capacity of U(VI) at equilibrium time and contact time t [min], respectively, and k_1 [min^{-1}] represents the pseudo first order kinetic constant. q_e and k_1 can be calculated from the slope and intercept of the plot of log (q_e-q_t) versus t, respectively (Figure S4A).

Pseudo-second-order model is expressed as the following Equation (2):

$$\frac{t}{q_t} = \frac{1}{k_2 \times q_e^{\,2}} + \frac{t}{q_e} \qquad (2)$$

where k_2 [g/mg/min] represents the rate constant of the pseudo-second order model, and can be determined from the plot of t/q_t against t (Fig. S4B).

Sorption isotherms. Langmuir model can be described as Equation (3):

$$\frac{C_e}{q_e} = \frac{1}{q_{max} b} + \frac{C_e}{q_{max}} \qquad (3)$$

where b [L mg^{-1}] is the Langmuir constant related to the affinity of binding sites, and q_{max} [mg g^{-1}] is the maximum sorption capacity. They can be calculated from the linear plot of C_e/q_e against C_e (Fig. S5A).

The Freundlich model[1] is applied for multilayer sorption, which can be described as Equation (4):

$$\log q_e = \log K_F + \frac{1}{n} \log C_e \qquad (4)$$

where K_F [mg/g $(L/mg)^{1/n}$] and n are the Freundlich constants related to sorption capacity and sorption intensity, respectively, which can be calculated from the linear plot of log q_e versus log C_e (Fig. S5B).

Thermodynamic studies. Three basic thermodynamic parameters, free energy change (ΔG), enthalpy change (ΔH) and entropy change (ΔS), were calculated according to Equation (5) and (6).[4, 5]

$$\ln K_a = \frac{\Delta S}{R} - \frac{\Delta H}{RT} \qquad (5)$$

$$\Delta G = \Delta H - T\Delta S \qquad (6)$$

where K_a is the thermodynamic attachment equilibrium constant, which is numerically equal to the Langmuir equilibrium constant b for neutral adsorbates or adsorbates with very weak charge.[6] R = 8.3145 [J (mol·K)$^{-1}$] is the universal gas constant, and T [K] is the absolute temperature. According to Equation (5), the plot of ln K_a vs. 1/T (Fig. S9) can give the value of ΔS [J (mol·K)$^{-1}$] and ΔH [kJ mol^{-1}], and according to Equation (6) can get ΔG (kJ mol^{-1}).

Distribution ratio (K_d). The distribution ratio (K_d) [L/g] is calculated according to Equation (7):

$$K_d = \frac{C_0 - C_e}{C_e} \times \frac{V}{M} \qquad (7)$$

where C_0 and C_e [mg L^{-1}] are the initial and equilibrium concentration of uranyl ions, respectively. M [g] is the weight of sorbent, and V [L] is the volume of the testing solution.

Table S1. Concentrations of various elements in testing solution.

Element	Total valence ions in 6M HNO_3 solution[a]	Conc. of metal ions in Simulated solution (ppm)
$UO_2(NO_3)_2{\cdot}6H_2O$	$UO_2NO_3^+$	105.1
$NaNO_3$	Na^+	165.1
$Nd(NO_3)_3$	$NdNO_3^{2+}$	88.1
$Gd(NO_3)_3{\cdot}6H_2O$	$GdNO_3^{2+}$	175.4
$La(NO_3)_3{\cdot}6H_2O$	$LaNO_3^{2+}$	99.0
$CeCl_3{\cdot}7H_2O$	$CeNO_3^{2+}$	100.0
$ZrCl_4$	$ZrOH_3^+$	99.4
$SrCl_2{\cdot}6H_2O$	$SrNO_3^+$	144.7
$CsNO_3$	Cs^+	13.5
$Ba(NO_3)_2$	$BaNO_3^+$	105.1
$Ni(NO_3)_2{\cdot}6H_2O$	Ni_2^+	108.8
$CrCl_3{\cdot}6H_2O$	Cr^{3+}	103.0
$CoCl_2$	Co^{2+}	138.9
$ZnCl_2$	Zn^{2+}	109.8
$Sm(NO_3)_3{\cdot}6H_2O$	$SmNO_3^{2+}$	47.6

a: Metal species in nitric acid solution simulated by Medusa program. ([M] = concentration of metal ions in 6 M nitric acid)

Table S2. BET surface areas, pore volumes, pore diameter and microanalysis of networks synthesized in different conditions

	1 M Na_2CO_3 solution content[1]	Temperature (°C)	Surface area (m^2 g^{-1})	Pore diameter (nm)[2]
CMP-H1	5%	90 °C for 1 days, 120 °C for 3 days	40.9	4.5
CMP-H2	10%	90 °C for 1 days, 120 °C for 3 days	100.6	3.2
CMP-H3	20%	90 °C for 1 days, 120 °C for 3 days	20.5	2.8
CMP-H4	10%	90 °C for 1 days, 150 °C for 3 days	25.9	1.4
CMP-H5	10%	100°C for 4 days	48.8	3.2

1: percent of DMF (V/V); 2: calculated by the nonlocal density functional theory (NLDFT) method.

Table S3. XPS Binding Energies, Fitting Parameters fwhm and content for CMP-EP.

Element	Assignment	Binding energy (eV)	FWHM*	Content (%)
O (1s)	P=O	533.0	1.81	66.7
	P-O	531.8	1.92	33.3
P (2p) (1/2)	PO_3	134.0	1.23	33.0
P (2p) (3/2)	PO_3	133.2	1.22	67.0

*: FWHM： full width at half maximum

Table S4. Kinetic parameters for the sorption of U(VI) by CMP-EP. (Experimental conditions: $C_{CMP\text{-}EP}$ = 1.0 mg mL^{-1}, $C_{U\ (VI)}$ = 4×10^{-5} mol L^{-1}, C_{HNO3} = 6 mol L^{-1}, and 298.15 K)

Temperature		Pseudo-first-order			Pseudo-second-order		
	$q_{e,exp}$ (mg/g)	k_1 (min^{-1})	$q_{e,cal}$ (mg/g)	R^2	k_2 (g/min/mg)	$q_{e,cal}$ (mg/g)	R^2
298 K	13.7	0.010	2.00	0.543	0.046	13.2	0.998
308 K	9.64	0.022	2.01	0.694	0.047	9.48	0.997
318 K	8.88	0.030	2.22	0.814	0.051	8.87	0.997

Table S5. Langmuir and Freundlich parameters for uranium (VI) sorption on CMP-EP. (Experimental conditions: $C_{CMP\text{-}EP}$ = 1.0 mg mL^{-1}, $C_{U\ (VI)}$ = 4×10^{-5} mol L^{-1}, C_{HNO3} = 6 mol L^{-1}, and 298.15 K)

Temperature	Langmuir model			Freundlich model		
	$q_{max,cal}$ (mg/g)	b (L/mg)	R^2	K_F (mol^{1-n} L^n/g)	n	R^2
298 K	73.1	0.099	0.996	3.42	2.05	0.927
308 K	63.2	0.089	0.993	3.22	2.12	0.913
318 K	56.2	0.066	0.994	2.88	2.04	0.917

Table S6. Thermodynamic parameters for uranium adsorption on CMP-EP.

ΔH (KJ/mol)	ΔS (J/mol K)	ΔG (kJ/mol)		
		298 K	308 K	318 K
-15.58	43.62	-28.56	-29.02	-29.45

Table S7. Comparison of sorption capacity and irradiation stability on various porous sorbents in acidic condition.

Matrix	Acidity	q_{max} (mg g^{-1})	k_2 (g mg^{-1} min^{-1})	Irradiation stability	Ref.
Phosphonate-Functionalized Mesoporous Carbon	pH 4.0	< 10	0.00816	-	7
Phosphazene-based COF	pH 1.5	124	0.0019	-	8
Phosphonate-functionalized ion-imprinted mesoporous silica	1 M HNO_3	80	0.108	500 kGy	9
Alkylphosphine oxides functionalized mesoporous silicas	2 M HNO_3	13.4	0.003	-	10
Mesoporous silica adsorbents bearing phosphonic acid	2 M HNO_3	<40	-	500 kGy	11
Polyetherether ketone with blended Cyanex 923	3 M HNO_3	<60	-	-	12
Merrifield chloromethylated resin with octyl(phenyl)-N,N-diisobutylcarbamoyl-methylphosphine oxide	4 M HNO_3	228.5	-	-	13
Phosphonic acid functionalized nanoporous polymer	4 M HNO_3	100.6	0.00388	-	14
Conjugated microporous polymers bearing phosphonate ligands	6 M HNO_3	73	0.046	1,000 kGy	This work

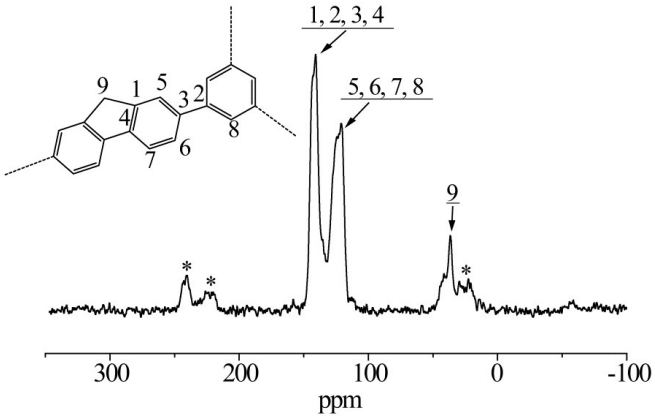

Fig. S1 Solid-state ^{13}C NMR spectra of CMP-H.

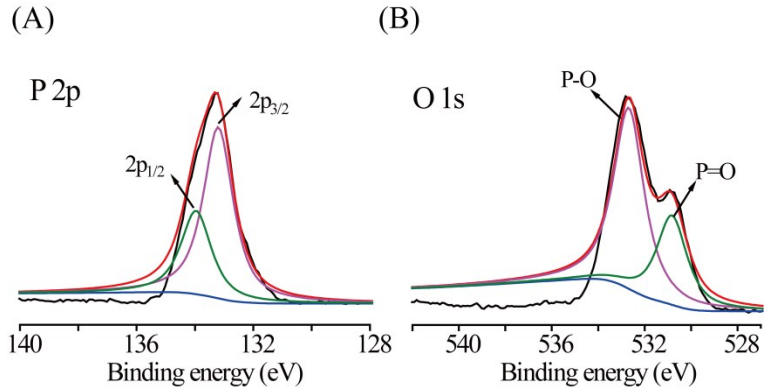

Fig. S2 XPS (A) P 2p and (B) O 1s spectra of CMP-EP.

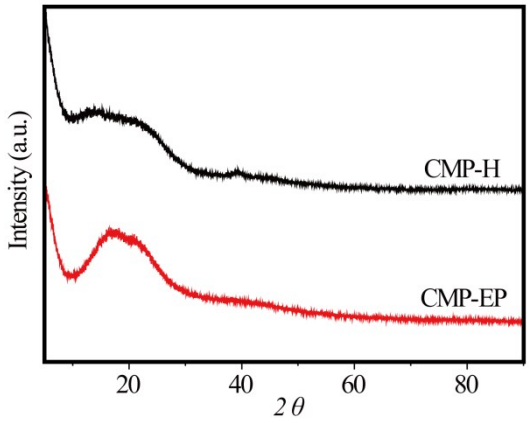

Fig. S3 Power X-ray diffraction (PXRD) pattern of CMP-H2 and CMP-EP.

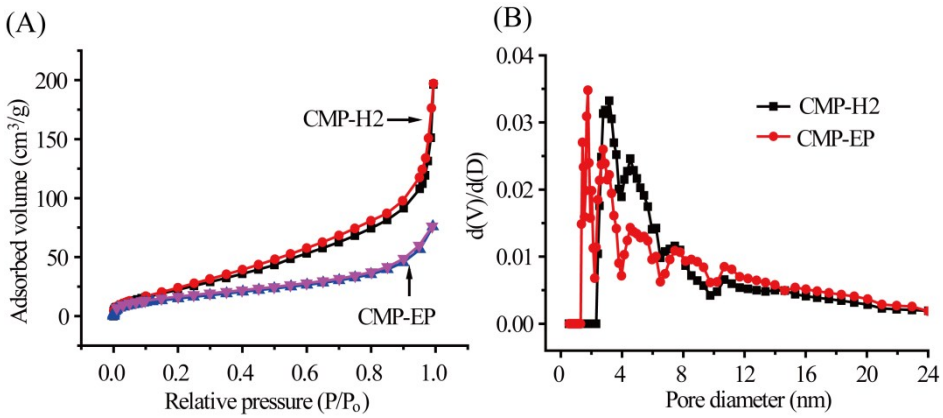

Fig. S4 (A) Nitrogen sorption/desorption isotherms and (B) pore size distribution for CMP-H2 and CMP-EP.

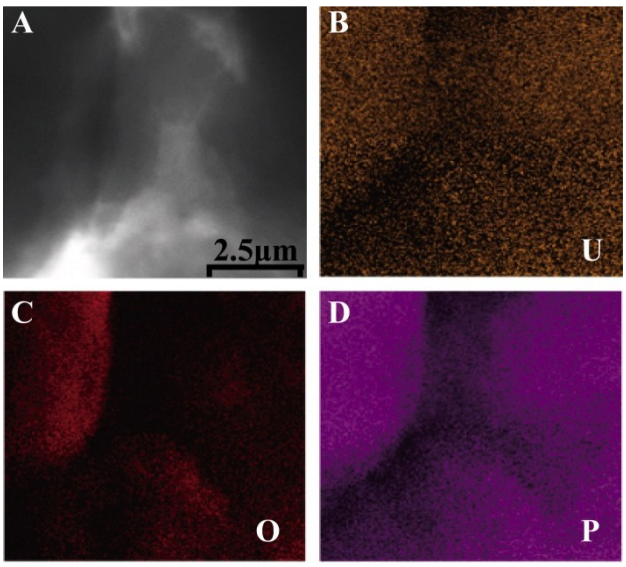

Fig. S5 (A) HAADF-STEM image, (B) uranium, (C) oxygen, and (D) phosphorus elemental mapping of the CMP-EP-U(VI).

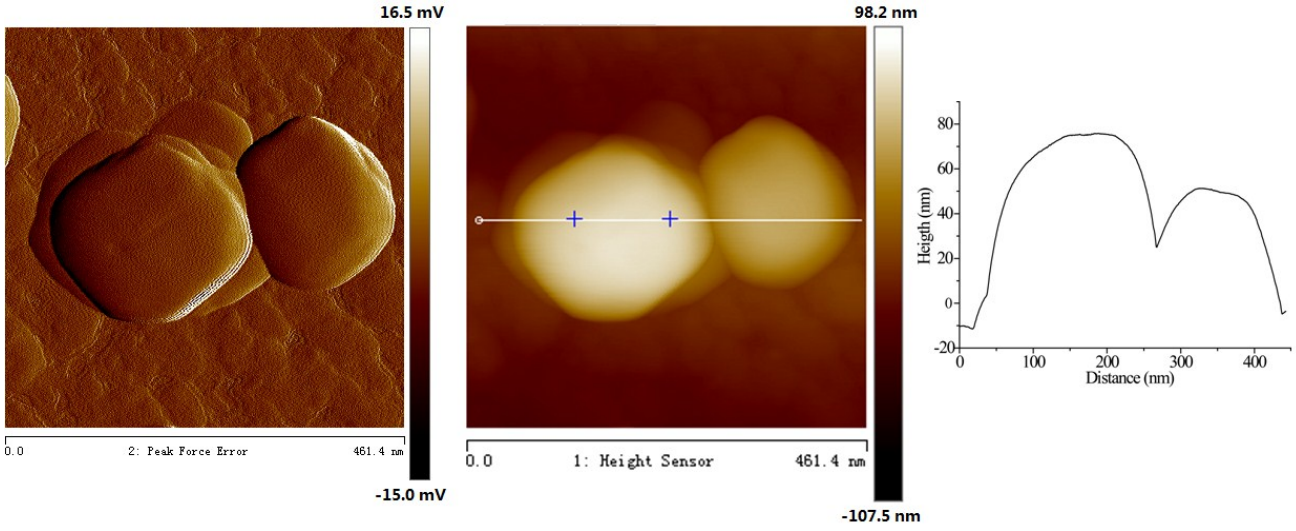

Fig. S6 AFM topography and height images, and line analysis of CMP-EP flakes dispersed on mica.

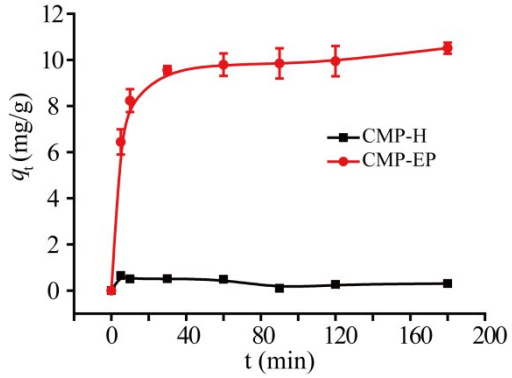

Fig. S7 Sorption Kinetics of CMP-PE and CMP-H2 for U(VI) at 298 K. (Experimental conditions: $C_{CMP\text{-}EP}$ = 1.0 mg mL^{-1}, $C_{U\ (VI)}$ = 4×10^{-5} mol L^{-1}, C_{HNO3} = 6 mol L^{-1})

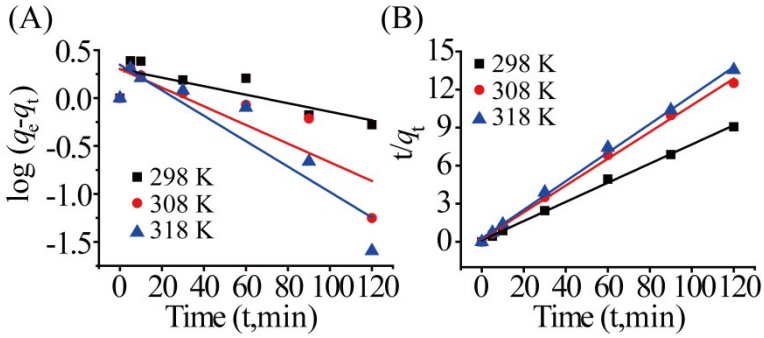

Fig. S8 (A) Pseudo-first order kinetics and (B) Pseudo-second order kinetics of uranium (VI) sorption on CMP-EP at 298, 308, and 318 K. (Experimental conditions: $C_{CMP\text{-}EP}$ = 1.0 mg mL^{-1}, $C_{U\ (VI)}$ = 4×10^{-5} mol L^{-1}, C_{HNO3} = 6 mol L^{-1})

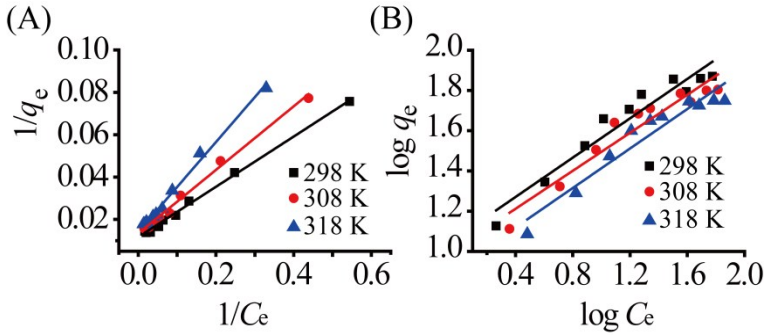

Fig. S9 (A) Langmuir model and (B) Freundlich model of uranium (VI) sorption on CMP-EP at 298, 308, and 318 K. (Experimental conditions: $C_{CMP\text{-}EP}$ = 1.0 mg mL^{-1}, $C_{U\ (VI)}$ = 4×10^{-5} mol L^{-1}, C_{HNO3} = 6 mol L^{-1})

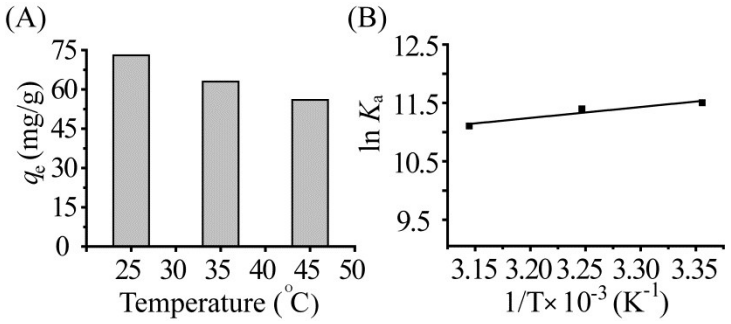

Fig. S10 (A) The maximum uranium sorption capability (q_{max}) of CMP-EP at different temperatures. (Experimental conditions: $C_{CMP\text{-}EP}$ = 1.0 mg mL^{-1}, $C_{U\ (VI)}$ = 4×10^{-5} mol L^{-1}, C_{HNO3} = 6 mol L^{-1}) (B) Linear plot of ln *K*a versus 1/T.

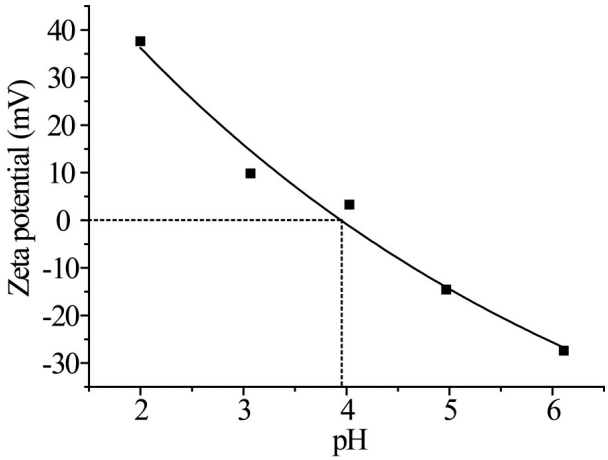

Fig. S11 Zeta potential of CMP-EP.

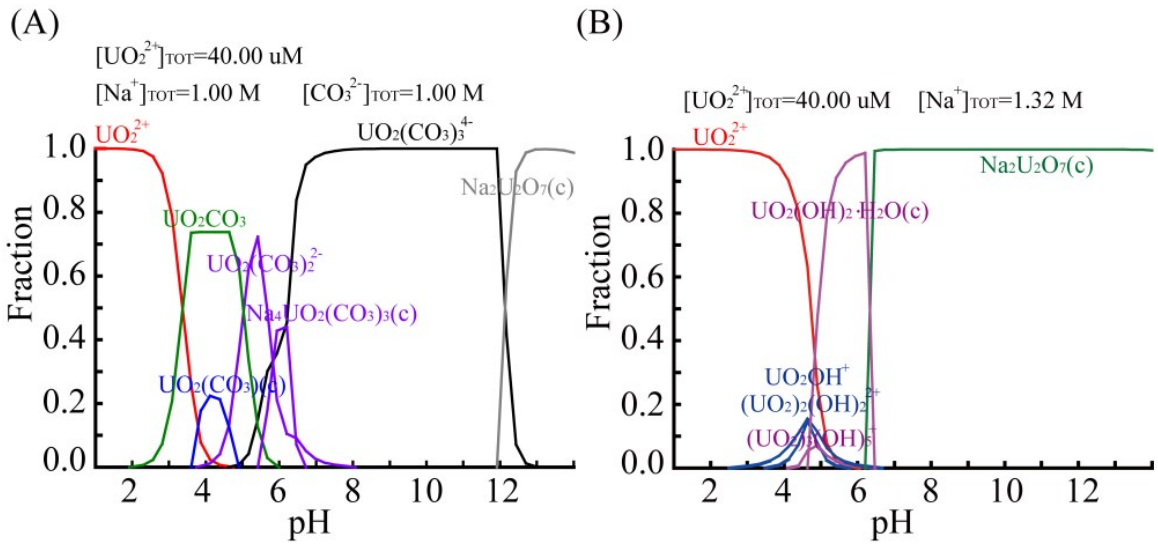

Fig. S12 Distribution of U(VI) species in aqueous solution ([U] = 0.04 mmol L^{-1} and pH values ranging from 1 to 14), which was simulated by Medusa program.

References:

1. B. Liu, B. S. Gaylord, S. Wang and G. C. Bazan, *Journal of the American Chemical Society*, 2003, **125**, 6705.
2. C. Chi, A. Mikhailovsky and G. C. Bazan, *Journal of the American Chemical Society*, 2007, **129**, 11134.
3. M. I. Mangione, R. A. Spanevello, A. Rumbero, D. Heredia, G. Marzari, L. Fernandez, L. Otero and F. Fungo, *Macromolecules*, 2013, **46**, 4754.
4. E. Oguz, *Journal of Colloid and Interface Science*, 2005, **281**, 62.
5. A. Mellah, S. Chegrouche and M. Barkat, *Journal of Colloid and Interface Science*, 2006, **296**, 434.
6. Y. Liu, *Journal of Chemical & Engineering Data*, 2009, **54**, 1981.
7. M. Carboni, C. W. Abney, K. M. L. Taylor-Pashow, J. L. Vivero-Escoto and W. Lin, *Industrial & Engineering Chemistry Research*, 2013, **52**, 15187.
8. S. Zhang, X. Zhao, B. Li, C. Bai, Y. Li, L. Wang, R. Wen, M. Zhang, L. Ma and S. Li, *Journal of Hazardous Materials*, 2016, **314**, 95.
9. S. Yang, J. Qian, L. Kuang and D. Hua, *ACS applied materials & interfaces*, 2017, **9**, 29337.
10. W. Zhang, G. Ye and J. Chen, *RSC Advances*, 2016, **6**, 1210.
11. W. Zhang, G. Ye and J. Chen, *Journal of Radioanalytical and Nuclear Chemistry*, 2016, **307**, 1445.
12. R. B. Gujar, D. S. Lakshmi, A. Figoli and P. K. Mohapatra, *Journal of Chromatography A*, 2013, **1305**, 48.
13. C. Siva Kesava Raju and M. S. Subramanian, *Journal of Hazardous Materials*, 2007, **145**, 315.
14. D. Yuan, Y. Wang, Y. Qian, Y. Liu, G. Feng, B. Huang and X. Zhao, *Journal of Materials Chemistry A*, 2017, **5**, 22735.